Cancer Research

# Stress Chaperone Mortalin Contributes to Epithelial-to-Mesenchymal Transition and Cancer Metastasis

Youjin Na[1,2], Sunil C. Kaul[1], Jihoon Ryu[1], Jung-Sun Lee[2], Hyo Min Ahn[1,2], Zeenia Kaul[3], Rajkumar S. Kalra[1], Ling Li[1], Nashi Widodo[4], Chae-Ok Yun[2], and Renu Wadhwa[1]

## Abstract

Mortalin/mthsp70 (HSPA9) is a stress chaperone enriched in many cancers that has been implicated in carcinogenesis by promoting cell proliferation and survival. In this study, we examined the clinical relevance of mortalin upregulation in carcinogenesis. Consistent with high mortalin expression in various human tumors and cell lines, we found that mortalin overexpression increased the migration and invasiveness of breast cancer cells. Expression analyses revealed that proteins involved in focal adhesion, PI3K–Akt, and JAK–STAT signaling, all known to play key roles in cell migration and epithelial-to-mesenchymal transition (EMT), were upregulated in mortalin-expressing cancer cells. We further determined that expression levels of the mesenchymal markers vimentin (VIM), fibronectin (FN1), β-catenin (CTNNB1), CK14 (KRT14), and hnRNP-K were also increased upon mortalin overexpression, whereas the epithelial markers E-cadherin (CDH1), CK8 (KRT8), and CK18 (KRT18) were downregulated. Furthermore, shRNA-mediated and pharmacologic inhibition of mortalin suppressed the migration and invasive capacity of cancer cells and was associated with a diminished EMT gene signature. Taken together, these findings support a role for mortalin in the induction of EMT, prompting further investigation of its therapeutic value in metastatic disease models. *Cancer Res; 76(9); 2754–65. ©2016 AACR.*



## Introduction

Recent progress in cancer diagnosis and treatment regimens has contributed to better treatment outcomes and survival. However, it is still complicated by metastasis and recurrence that are the foremost contributors of fatality. The process of metastasis, spread of cancer from one organ to the other, not connected to it directly, is facilitated by a number of steps including (i) acquisition of increased motility of proliferating tumor cells, (ii) their detachment from the primary tumor site, and (iii) travel to the secondary sites through extracellular matrix (ECM) and blood stream. The molecular mechanisms involved in metastasis have been shown to involve deregulation of the signaling pathways that control normal epithelial-to-mesenchymal transition (EMT). During this process, the epithelial cells lose their cell polarity and cell–cell adhesion (epithelial characteristics) and acquire migratory and invasive properties (mesenchymal characteristics) by multiple pathways; several of these are yet to be clarified. Shift in protein profiles and cytoskeleton characteristics are often considered as biomarkers of EMT. For example, cell surface proteins, E-cadherin (biomarker of epithelial cells), or integrins are replaced by mesenchymal markers (N-cadherin, vimentin, or fibronectin). These processes are driven by several regulatory proteins including key transcriptional factors, Snail, Slug, and Twist (1–4). Consistent with the enrichment of these transcription factors in tumors as compared with normal tissues, their ectopic expression has been shown to induce EMT, downregulation of E-cadherin, and increase in tumor metastasis (1). On the basis of these data, they have also been suggested as prognostic markers for cancer metastasis (5–7). Several signaling pathways including Ras-MAPK, TGFβ, EGF, FGF, FAK, and Wnt/β-catenin have been shown to activate Snail, Slug, and Twist transcription factors and regulate EMT (8–10). Active Wnt/β-catenin pathway causing upregulation of Snail and vimentin has been correlated with poor prognosis and advance stages of breast cancer. TGFβ that acts as a tumor suppressor at early stages of cancer has also been shown to promote malignant properties of tumors, including invasion and metastasis at the later stages. It is found enriched in breast cancer bone metastasis (11). p53, on the other hand, has been shown to repress EMT by transcriptional repression of SNAIL and noncoding regulation mediated by miRNAs (12). EMT has also been correlated with the drug resistance characteristics of cancer cells. Tamoxifen-resistant MCF-7 cells showed aggressive and invasive

[1]Drug Discovery & Assets Innovation Lab, DBT-AIST International Laboratory for Advanced Biomedicine (DAILAB), Biomedical Research Institute, National Institute of Advanced Industrial Science & Technology (AIST), Tsukuba, Japan. [2]Department of Bioengineering, College of Engineering, Hanyang University, Seoul, Korea. [3]Department of Molecular Virology, Immunology and Medical Genetics, The Ohio State University, Columbus, Ohio. [4]Department of Biology, Faculty of Mathematics and Natural Sciences, Brawijaya University, Malang, Indonesia.

**Note:** Supplementary data for this article are available at Cancer Research Online (http://cancerres.aacrjournals.org/).

Y. Na and S.C. Kaul are co-first authors of this article.

**Corresponding Authors:** Renu Wadhwa, National Institute of Advanced Industrial Science & Technology (AIST), Central 5-41, 1-1-1 Higashi, Tsukuba, Ibaraki - 305 8565, Japan. Phone: 81-29-861-9464; Fax: 81-29-861-2900; E-mail: renu-wadhwa@aist.go.jp; and Chae-Ok Yun, Department of Bioengineering, College of Engineering, Hanyang University, 222 Wangsinmi-ro, Seongdong-gu, Seoul - 04763, Republic of Korea. Phone: 82-2-2220-0491; Fax: 82-2-2220-4850; E-mail: chaeok@hanyang.ac.kr

**doi:** 10.1158/0008-5472.CAN-15-2704

behavior that could be reversed upon the inhibition of the autocrine EGFR pathway, also known to be involved in EMT (3, 13–15). Despite the wealth of existing data on the role of EMT in cancer metastasis, its clear picture, diagnostic, and therapeutic targets are yet to be clearly elucidated.

Stress chaperone mortalin/mthsp70 is an essential protein often enriched in cancer cells, and promotes their pro-proliferative characteristics by multiple pathways (16–19). It interacts with tumor suppressor protein p53 and inactivates its functions, including transcriptional activation and control of centrosome duplication leading to uncontrolled proliferation, a hallmark of cancer cells (19–22). Most recently, it was shown to activate telomerase and hnRNP-K proteins and contribute to malignant phenotype of cancer cells (23). In agreement with these reports, knockdown of mortalin in cancer cells was shown to activate p53 function and cause their growth arrest or apoptosis (17, 18, 24–27). Some studies have shown correlation of mortalin expression level with metastatic potential and tumor recurrence in case of hepatocellular carcinoma, suggesting clinical application of mortalin as a chemotherapeutic drug target (17, 28, 29). Chen and colleagues also showed that the genetically isogenic cell lines with variable metastatic potentials possess tight correlation with the level of expression of mortalin, suggesting its role in metastatic hepatocellular carcinoma (HCC; ref. 29). Furthermore, mortalin-compromised cells showed inhibition of EMT, suggesting mortalin as a therapeutic target for HCC metastasis, and hence warranted further studies.

We, in this study, examined the clinical relevance of mortalin in tumorigenesis and tumor progression using public cancer patient databases and commercially available tumor tissue samples. cDNA, miRNA, and antibody microarray analyses revealed upregulation of several EMT signaling proteins in mortalin-overexpressing breast cancer cells, both at the transcript and protein levels. Furthermore, these could be reversed by knockdown of mortalin, suggesting it to be a therapeutic target for cancer metastasis.

## Materials and Methods

### Materials

Antibodies were procured from different sources as follows: β-catenin, E-cadherin, and vimentin (Cell Signaling Technology); α smooth muscle actin (α-SMA; Abcam); hnRNP-K, MMP-2, MMP-3, and fibronectin (Santa Cruz Biotechnology); keratin 8 (OriGene Technologies); keratin 14 (Anaspec); keratin 18, myc-tag, and β-actin (Cell Signaling Technology), and Alexa Fluor 488-conjugated/568-conjugated secondary antibodies. Monoclonal anti-mortalin antibody (Clone C1–3) was raised in our laboratory. Hoechst 33342 (1 μg/mL) and tetramethylrhodamine isothiocyanate (TRITC)-conjugated phalloidin were from Sigma. Tumor tissues and microarray slides with clinical tumor samples (of diverse origin, histology, grades, and of differentiation status) and their matched normal controls were procured from Superbiochips Laboratories and BioChain Institute Inc.

### IHC

Paraffin-embedded tissues and tissue microarray slides were deparaffinized in xylene and stained with anti-mortalin antibody using Dako REAL EnVision Detection System as described previously (23). Images of mortalin staining in matched normal and tumor tissue were captured under a fluorescence microscope (BZ-9000, Keyence), using BZ-II Analyzer software (Keyence). Tissue sections incubated without anti-mortalin antibody were used as negative control. ImageJ software (NIH, Bethesda, MD) was used for quantification of mortalin expression in acquired images.

### The Cancer Genome Atlas and Human Protein Atlas analysis

Information on mortalin (HSPA9) genetic alterations, patient survival, and expression levels (mRNA expression, z score, threshold -1.5), mRNA expression analysis for Kidney RCCC dataset was performed with grade I, III, and IV tumors; grade II consisted of information of only one patient case and thus excluded from quantitation; $n$ = number of patients, on omitting outliers (expressions fluctuating beyond threshold) with tumor progression (grades) was examined using The Cancer Genome Atlas (TCGA) http://www.cbioportal.org/index.do. Human Protein Atlas (HPA) http://www.proteinatlas.org, an antibody-based proteomic database was used to examine mortalin expression in normal and cancer tissues.

### Cell culture

Human normal (TIG-3; JCRB Cell Bank), cancer (breast epithelial, MCF7 and MDA-MB-231; osteosarcoma (DS Pharma Biomedical) and U2OS and melanoma, G361 (JCRB Cell Bank) were grown in DMEM (Life Technologies) as described previously (22, 23). Cells were authenticated by either STR-PCR or Isozyme analysis at the respective sources. The original cells were stocked (in multiple vials) in LN2 within five population doublings from the time of procurement (1–3 years for different cell lines). To avoid genetic instability due to prolonged cultures, cells were revived from the original stocks at times, as required, for the current study. Mortalin-overexpressing derivative cells were generated by mortalin encoding retroviral vector as described previously (16, 23). The stably infected cells were maintained in G418 (100 μg/mL) supplemented medium.

### Generating shMot-expressing adenoviral vectors

To generate an adenovirus-expressing shMot or shScr at the E3 regions, pdE1-RGD was linearized by *Spe*I digestion and cotransformed into *Escherichia coli* BJ5183 with the *XmnI*-digested pSP72-E3/CMV-shMot or pSP72-E3/CMV-shScr E3 shuttle vector (25) for homologous recombination, generating a dE1-RGD/shMot or dE1-RGD/shScr adenoviral vector. The propagation, purification, and titration of adenoviruses were performed as described previously (30).

### Cell proliferation assay

Cell proliferation was measured by MTT assay (DUCHEFA Biochemie). Cells were seeded in 48-well plates ($5 \times 10^3$ cells/well) and treated with either PBS, dE1-RGD/shScr or dE1-RGD/shMot (10, 20, 50, 100, 200 MOI) after 24 hours. Cell morphology and viability of control and virus-treated cells were also monitored every day under a microscope and by staining with crystal violet (0.5% in 50% methanol), respectively. All assays were performed independently, at least, three times.

### Migration and invasion assay

Cells were treated with PBS, dE1-RGD/shScr, or dE1-RGD/shMot (20–50 MOI) and plated on the top chamber ($5 \times 10^4$ cells/well) of Transwell chamber. FBS (10%) was placed in the bottom of Transwell chamber and the assembly was incubated at 37°C for 4 to 6 hours, fixed, and stained with hematoxylin and

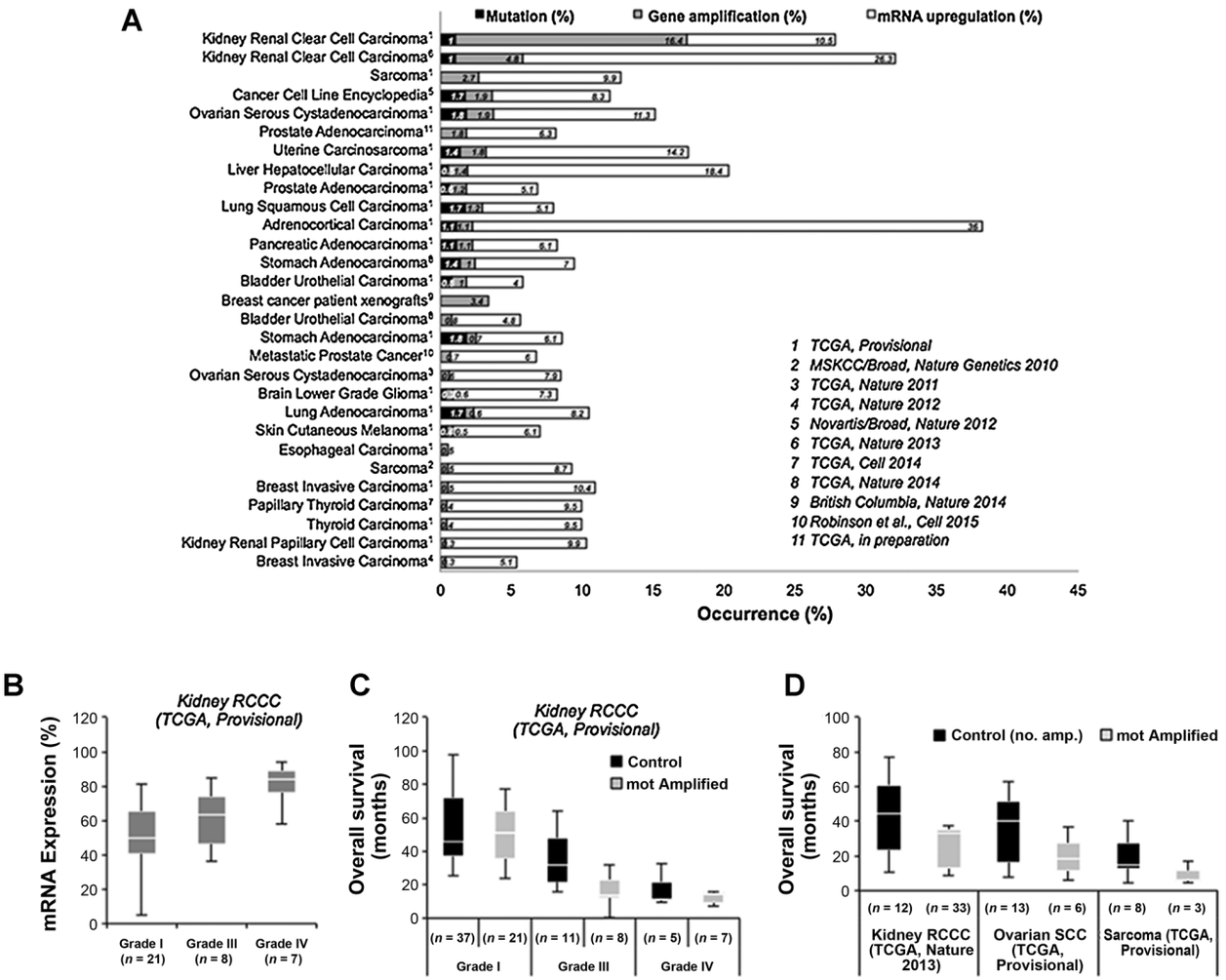


**Figure 1.**

Mortalin enrichment in tumors correlates with tumor progression and poor survival of patients. A, percentage occurrence of mortalin mutations, gene amplification, and mRNA upregulation observed in a number of TCGA clinical cancer datasets. B, enrichment of mortalin mRNA in advanced grade kidney-renal clear cell carcinoma (TCGA, provisional; $n$ = number of patients). C, quantitation showing overall survival of kidney-renal clear cell carcinoma (RCCC) patients with and without mortalin amplification. D, overall survival of patients with and without mortalin amplification in other tumor patient datasets (kidney-renal clear cell carcinoma; *Nature*, 2013, ovarian serous cystadenocarcinoma; TCGA, provisional and sarcoma; TCGA provisional) are shown.

eosin (23). *In vitro* Matrigel invasion assays were performed using BD BioCoat Matrigel Invasion Chamber (BD Biosciences) following the manufacturer's instructions and as described previously (23).

### Wound-healing assay

Cells grown in monolayer were scratched straight by a 100-μL pipette-tip followed by washing with PBS and culture in normal medium. The time of scratch was designated as 0 hour and cells were allowed to migrate into the gap. Movement of cells to the scratch area was followed for the next 24 to 48 hours. Images were acquired under the phase contrast microscope (Nikon) with a 10× phase objective lens at 0, 24, and 48-hour time points. For shRNA experiments, equal number ($5 \times 10^4$ cells/well) of cells were plated on 12-well plates and then treated with dE1- RGD/shScr or dE1- RGD/shMot (20–50 MOI). After 48 hours, straight-line scratch was made and followed by microscopic observations at 0, 3, 6, and 16 hours. The WimScratch software (Wimasis) was used for analysis of captured images in shRNA experiments. Wound-healing activity is expressed as percentage filling of scratched area from three independent experiments.

### cDNA, miRNA, and antibody array analyses

Control- and mortalin-overexpressing cells were harvested at 80% confluency. For miRNA microarray, small RNAs (less than 200 nt including precursor and mature miRNAs) were extracted using mirVana miRNA Isolation Kit (Ambion) following the manufacturer's protocol. Purified RNA was labeled with Cy3 or Cy5 using the mirVana miRNA labeling kit (Ambion). Labeled RNA was hybridized with miRNAs arrayed on slides (Hokkaido-System Science), and detected by a scanner (Agilent Technologies).

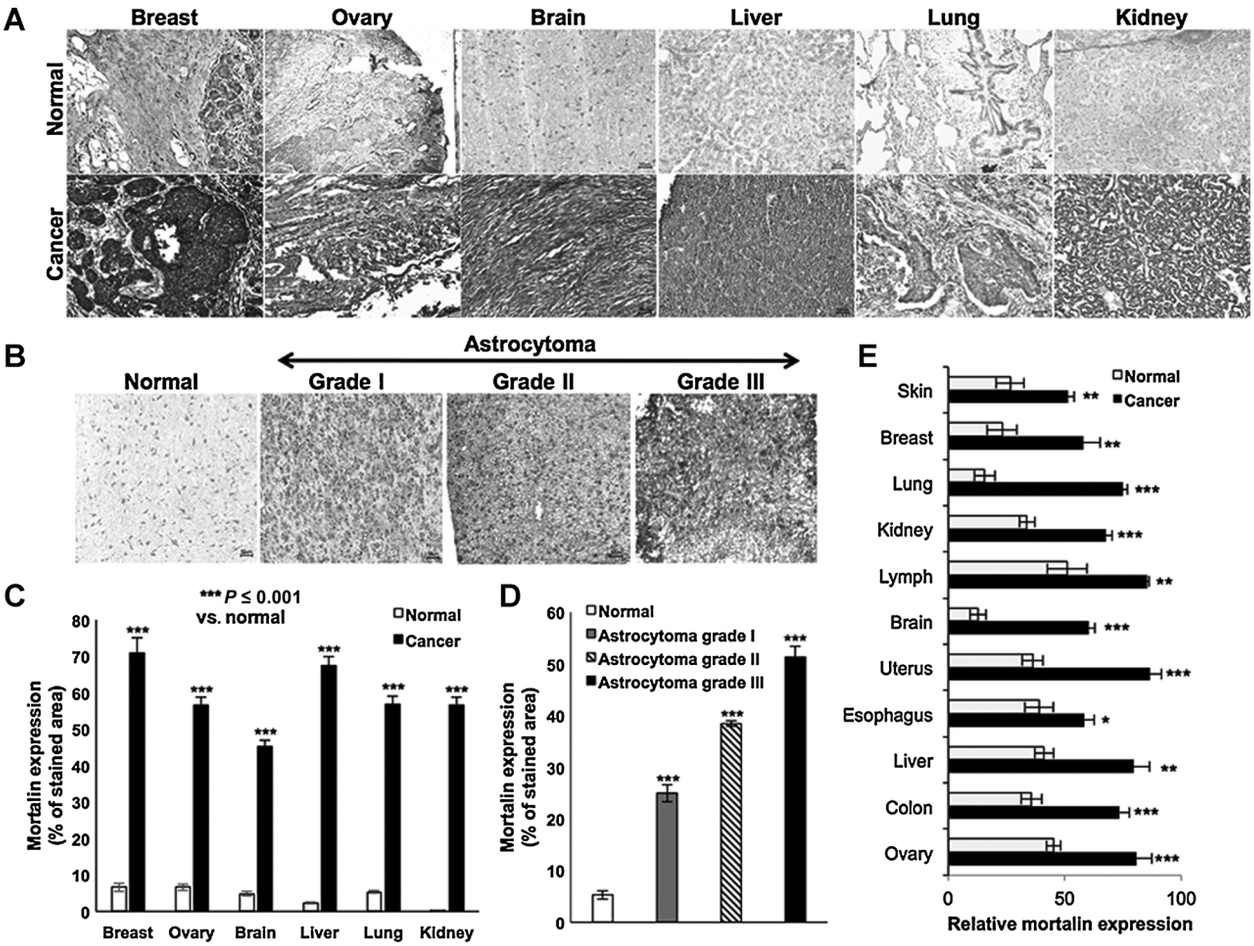


**Figure 2.**

Upregulation of mortalin in tumor tissues. Normal (control) and matched tumor tissues were stained with anti-mortalin antibody. Increased expression of mortalin in tumors (A and C) and its correlation with tumor aggressiveness (B and D). E, upregulated mortalin expression in a variety of tumors as compared with their normal tissue controls, as detected on tissue microarray slide. Quantitative analysis was performed using ImageJ software. All results are shown as mean ± SE. *, $P < 0.05$; **, $P < 0.01$; ***, $P < 0.001$ compared with normal. Original magnification, ×200.

For cDNA array, total RNA was prepared using TRIzol reagent (Gibco BRL) following manufacturer's instructions, and labeled with Cy3 or Cy5 using Low Input Quick Amp Labeling Kit, Agilent Technologies, hybridized to human cDNA array slides and analyzed using Agilent 2100 BioAnalyzer series II (Hokkaido-System Science).

Antibody membrane array containing antibodies to growth factors and proteins involved in metastasis (Abcam) was used. Cell lysates and conditional medium from control and mortalin-overexpressing cells were prepared at 80% confluency. Lysate/conditional medium (collected and centrifuged at 3,000 rpm to remove cell debris) was incubated with the Human Growth Factor Antibody Array membrane following manufacturer's instructions and reagents provided in the kit. The membranes were developed using Universal hood II (Bio-Rad) and the intensities of blots were analyzed with Image Lab software.

miRNA array data were analyzed on the miRNA targets predicted by mirPath, DIANA-microT-CDS, and combined with meta-analysis using the Kyoto Encyclopedia of Genes and Genomes (KEGG) databases (31–34) using software from DIANA Laboratory. The results of the analysis were presented on the chart based on the *P* value, targeted genes, and number of miRNAs that were actively involved in the pathway. The array data were analyzed using Gene Annotation Tool to help explain relationships (Gather; ref. 32) and Advaita Bio's iPathway Guide (http://www.advaitabio.com/ipathwayguide). The software analysis tool implemented the "Impact Analysis" approach that took into consideration the direction and type of all signals on a pathway, the position, role, and type of the genes (33). The genes were plotted in KEGG pathway database (34).

### Western blotting

Cells were lysed using 1% Nonidet P-40 buffer containing a protease inhibitor cocktail (Sigma Aldrich), and subjected to Western blotting as described previously (22, 23) using specific antibodies as indicated above.

### Immunofluorescence assay

For immunofluorescence microscopy, cultured cells were washed with PBS, fixed in 4% paraformaldehyde for 10 minutes

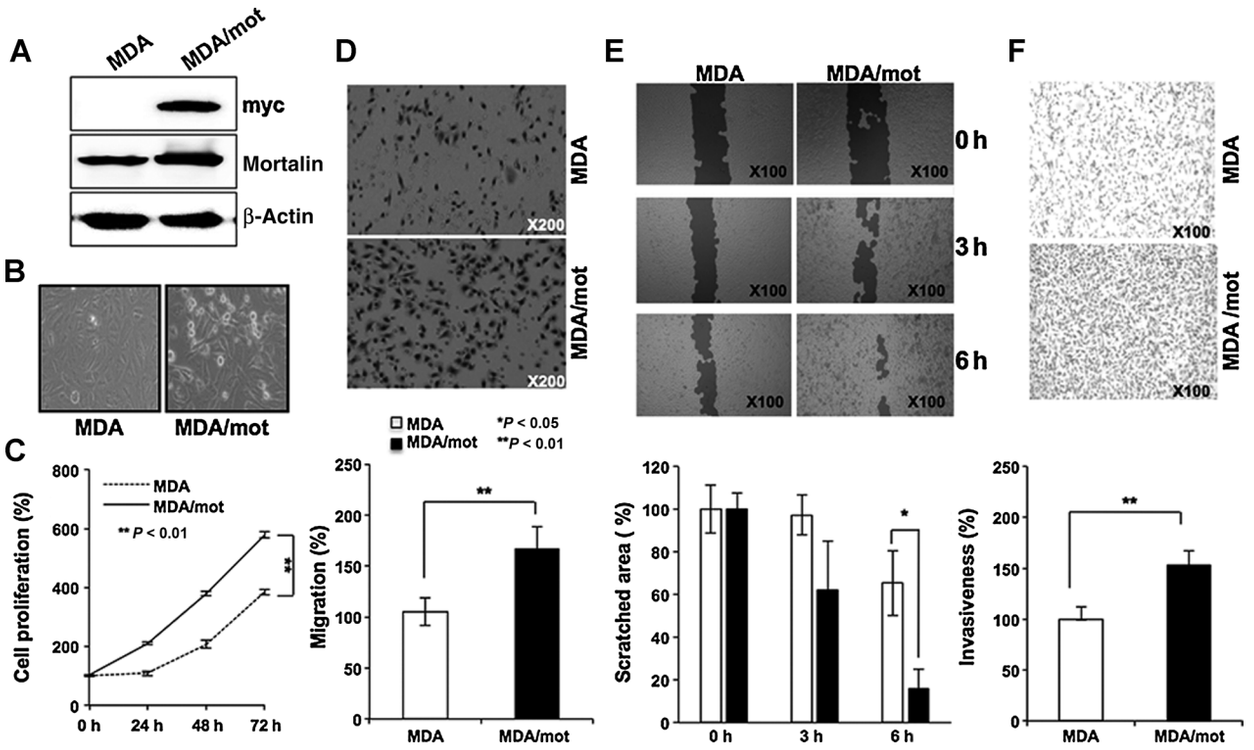


**Figure 3.**
Mortalin-overexpressing cells showed increase in migration and invasion properties. Mortalin-overexpressing MDA-MB-231 (MDA) cells (A) showed change in cell morphology (B), increase in cell proliferation (C), migration (D and E), and invasion (F) capacities. Data are presented as mean±SE ($n = 3$). *, $P < 0.05$; **, $P < 0.01$ compared with MDA.

at room temperature, and permeabilized by 0.1% Triton X-100 in PBS for 15 minutes. Fixed cells, blocked with 1% BSA, were incubated with primary antibodies (as indicated), washed, and visualized by secondary antibodies (Alexa Fluor 488–conjugated anti-rabbit IgG or Alexa Fluor 568–conjugated anti-mouse IgG) as described previously (22, 23). TRITC-conjugated phalloidin and Hoechst 33342 (both at 1 μg/mL, Sigma) were used for actin and for nuclear staining, respectively. The cells were viewed under a confocal laser scanning microscope (LSM510, Carl Zeiss Micro Imaging).

### MMP-2 ELISA

MMP-2 ELISA was performed using SensoLyte520 MMP-2 Assay Kit (Anaspec) following the manufacturer's instructions. Cells were seeded in 6-well plates ($1 \times 10^5$ cells/well), and supernatants were collected at 48 hours after incubation at 37°C. The fluorescence intensity was read using a SpectraMax M2 plate reader (Molecular Devices) with 490/520 nm filter set.

### Reverse transcription (RT)-PCR and real-time PCR

Total RNA from cultured cells was prepared with TRIzol reagent (Gibco BRL). Complementary DNA was prepared from 1 μg total RNA by random priming using a First-Strand cDNA Synthesis Kit (Promega Corp.) as described previously (23). For real-time PCR, first-strand cDNA synthesis and real-time PCR were performed using QuantiTect Reverse Transcription Kit (Qiagen) and Eco Real-Time PCR System (Illumina; ref. 23). The sequence of the primers were as follows: 18S; forward primer 5′-AACCCGTTGAACCCCATT-3′ and reverse primer 5′-CCATCCAATCGGTAGTAGCG-3′; mortalin, forward primer 5′-AGCTGGAATGGCCTTAGTCAT-3′ and reverse primer 5′-CAGGAGTTGGTAGTACCCAAATC-3′; β-catenin, forward primer 5′- AAAGCGGCTGTTAGTCACTGG-3′ and reverse primer 5′-GACTTGGGAGGTATCC ACATCC-3′; E-cadherin, forward primer 5′- CGGGAATGCAGTTGAGGATC-3′ and reverse primer 5′- AGGATGGTGTAAGCGATGGC-3′; vimentin, forward primer 5′- CCTTGAACGCAAAGTGGAATC-3′ and reverse primer 5′- GACATGCTGTTCCTGAATCTGAG-3′; α-SMA, forward primer 5′- CCGACCGAATGCAGAAGGA-3′ and reverse primer 5′- ACAGATATTTGCGCTCCGAA-3′; fibronectin, forward primer 5′-GGAGAATTCAAGTGTGACCCTCA-3′ and reverse primer 5′- TGCCACTGTTCTCCTACGTGG-3′; VEGF, forward primer 5′-CTACCTCCACCATGCCAAGT-3′ and reverse primer 5′-GCAGTAGCTGCGCTGATAGA-3′; MMP-2, forward primer 5′-TACAGGATCATTGGCTACACACC-3′, and reverse primer 5′-GGTCACATCGCTCCAGACT-3′; MMP-3, forward primer 5′-ATTCCATGGAGCCAGGCTTTC-3′ and reverse primer 5′-CATTTGGGTCAAACTCCAACTGTG-3′; MMP-7, forward primer 5′-GAGTGAGCTACAGTGGGAACA-3′ and reverse primer 5′-CTATGACGCGGGAGTTTAACAT-3′; MMP-9, forward primer 5′-TGTACCGCTATGGTTACACTCG-3′ and reverse primer 5′-GGCAGGGACAGTTGCTTCT-3′; hnRNP-K, forward primer 5′-AGCAGAGCTCGGAATCTTCCTCTT-3′ and reverse primer 5′-ATCAGCACTGAAACCAACCATGCC-3′; CK8, forward primer 5′-CAGAAGTCCTACAAGGTGTCCA-3′ and reverse primer 5′-CTCTGGTTGACCGTAACTGCG-3′; CK18, forward primer 5′-CACAGTCTGCTGAGGTTGGA-3′ and reverse primer 5′-

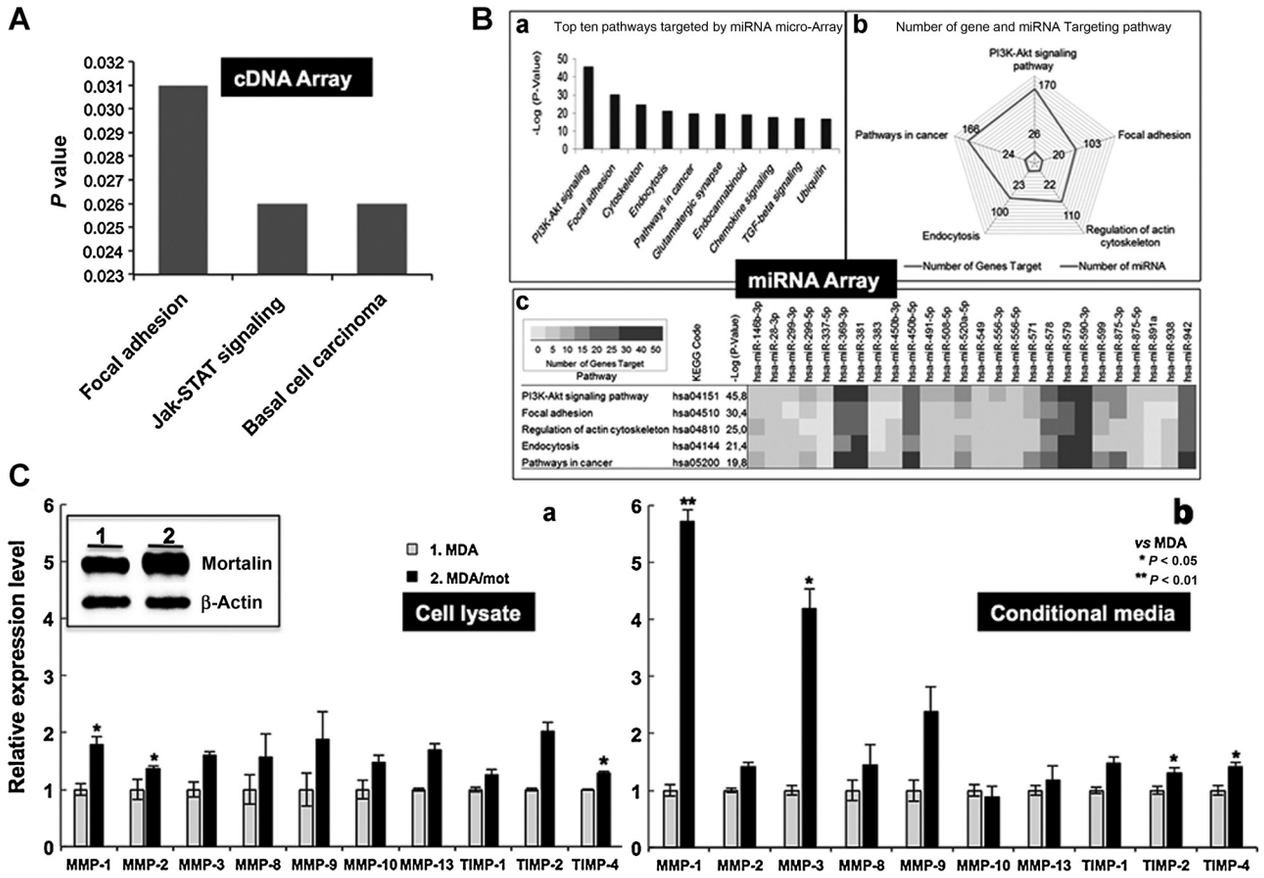


**Figure 4.**
Mortalin-overexpressing cells showed upregulation of proteins involved in EMT and metastasis signaling. cDNA (A) and miRNA microarray analysis (B) of control and mortalin-overexpressing MDA cells revealed upregulation of focal adhesion, PI3K–Akt, cytoskeleton, and TGFβ signaling in the latter. The top five pathways upregulated by miRNA depletion in mortalin-overexpressing cells are shown (B, a–c). C, upregulation of proteins (a) involved in cell migration and metastasis and their secretion (b) as detected by antibody membrane array is shown. Data are presented as mean ± SE ($n = 2$). *, $P < 0.05$; **, $P < 0.01$ compared with control MDA cells.

CAAGCTGGCCTTCAGATTTC-3′; Wnt-3α, forward primer 5′-CAAGATTGGCATCCAGGAGT-3′ and reverse primer 5′-TCCCTGGTAGCTTTGTCCAG-3′; and TGFβ, forward primer 5′-CAATTCCTGGCGATACCTCAG-3′ and reverse primer 5′-GCACAACTCCGGTGACATCAA-3′.

### Statistical analysis

Results are expressed as mean ± SD. Group results were compared by one-way ANOVA, followed by *post hoc* Student *t* test for unpaired observations or Bonferroni correction for multiple comparisons when appropriate. $P < 0.05$ was considered significant.

## Results

### Overexpression of mortalin enhanced the migration and invasion potential of MDA-MB-231 cells

To explore the clinical relevance of the role of mortalin in carcinogenesis, we surveyed cancer patient database, TCGA, and found that mortalin/HSP9A gene locus and mRNA expression were frequently amplified in cancer patients; upregulation of mRNA was most frequent. On the other hand, mutations occur only rarely and most of them were functionally insignificant (Fig. 1A). Examination of the tumor database with information on mRNA expression and tumor grades (kidney-renal clear cell carcinoma; grades I, III, and IV) exhibited its positive association with tumor grades (Fig. 1B) and negative correlation with patient survival (Fig. 1C). Of note, decreased survival was also recorded in patients with mortalin amplification as compared with the ones without amplification in a number of other tumor datasets (Fig. 1D). Furthermore, the expression of mortalin was seen to upregulate with the aggressiveness of cancer- and stage-dependent manner in several tumor types, as validated by tissue microarray. For example, (i) grade III invasive breast carcinoma exhibited higher level of expression as compared with the grade II (Supplementary Fig. S1A), (ii) poorly differentiated aggressive lung tumors showed high level of mortalin expression as compared with the differentiated tumors (Supplementary Fig. S1B), and (iii) melanomas showed higher level of expression as compared with osteosarcoma and carcinoma (Supplementary Fig. S1C). In line with the above information, survey of public HPA database revealed that mortalin protein is enriched in tumors as compared with their normal tissue controls (Supplementary Fig. S1D), and consistent with the mRNA database information, it showed

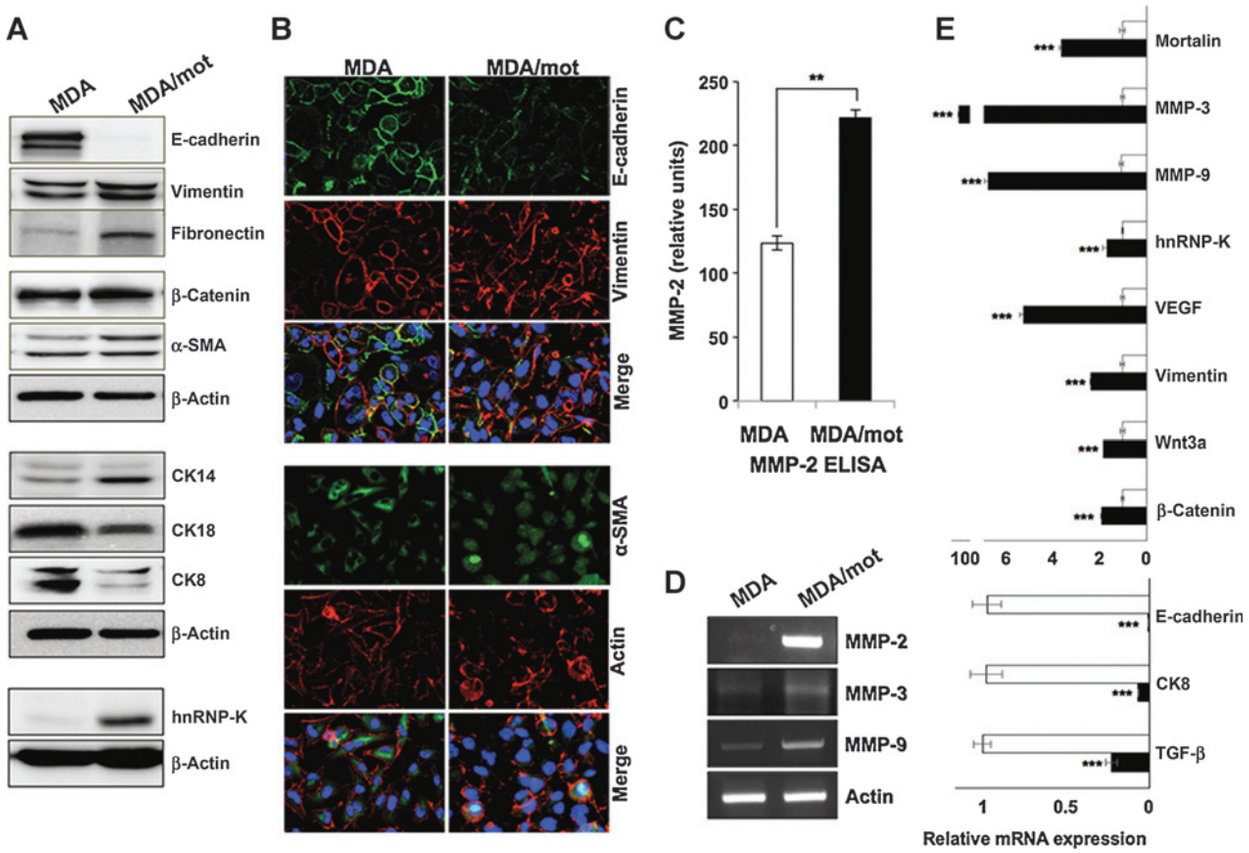


**Figure 5.**

Mortalin-overexpressing cells showed increase in proteins involved in EMT at protein and transcript level. A, Western blot analysis showing decrease in epithelial cell markers (E-cadherin, CK8, and CK18) and increase in mesothelial cell markers (vimentin, fibronectin, β-catenin, α-SMA, CK14, and hnRNP-K). B, immunostaining of control and mortalin-overexpressing cells showing decrease in E-cadherin and increase in vimentin and α-SMA. Actin was used as an internal control both for Western blotting and immunostaining. C and D, increased expression of MMP-2, as detected by ELISA (C) and RT-PCR (D). E, real-time qPCR assay of control and mortalin-overexpressing MDA cells showed increase in MMPs, hnRNP-K, VEGF, vimentin, and β-catenin. E-cadherin, CK8, and TGFβ showed decrease. Expression values are presented as mean±SE ($n = 3$). **, $P < 0.01$; ***, $P < 0.001$ compared with MDA.

higher expression level in melanoma than carcinoma tumors (Supplementary Fig. S1E). At this end, we also examined several tumor tissues and their matched controls for mortalin expression by IHC using commercial tumor tissue samples. As shown in Fig. 2A–D and data not shown, all the examined tumor tissue sections (breast fibroadenoma and invasive ductal carcinoma, ovarian teratoma, astrocytoma, hepatocellular carcinoma, squamous lung cell carcinoma, papillary renal cell carcinoma) and tissue microarray sections (skin, breast, lung, kidney, lymph, brain, uterus, esophagus, liver, colon, ovary cancer tissues) showed higher level of expression as compared with the control. Furthermore, aggressive tumors such as grade III astrocytoma showed higher level of expression as compared with the less aggressive grade I and II tumors (Fig. 2B and D). These data suggested that the overexpression of mortalin contributes to carcinogenesis and its progression to aggressive stages by multiple ways. It, therefore, possesses prognostic value and may serve as a therapeutic target.

On the basis of the above data, we predicted that mortalin might play a critical role in EMT and cancer metastasis. To define mechanisms, we first examined its expression level in a variety of cancer cells (Supplementary Fig. S2A). Four cell lines, A549, G361, MCF7, and MDA-MB-231 (MDA), with different level of expression were examined for their migration ability. We found a correlation between the level of mortalin expression and migration capacity of cells. A549 with highest level of expression among the four cell lines showed highest migration, G361 showed a moderate level, and MCF7 and MDA-MB-231 cells were slow as compared with the other two cell lines (Supplementary Fig. S2B and S2C), suggesting that mortalin may contribute to migration capacity of cancer cells. To investigate further, we selected MDA-MB-231 cells that possess moderate level of mortalin expression, and generated their mortalin-overexpressing derivatives by transduction with myc-tagged mortalin expressing retrovirus (Fig. 3A). Several clones were examined for the level of mortalin expression in MCF7/mot derivatives as described previously (23).They all were found to possess about 2- to 3-fold increase (23), and the current analysis was restricted to pooled cultures. The derivative MDA/mot cells showed somewhat rounded morphology (Fig. 3B), increased proliferation (Fig. 3C), migration (Fig. 3D and E), and invasion (Fig. 3F) capacities, as compared with the control vector–transfected cells. The difference in these phenotypes was statistically significant as analyzed by several independent experiments (Fig. 3D–F, bottom) in mortalin-overexpressing MDA as well as -MCF7 cells (data not shown). Electron microscopic

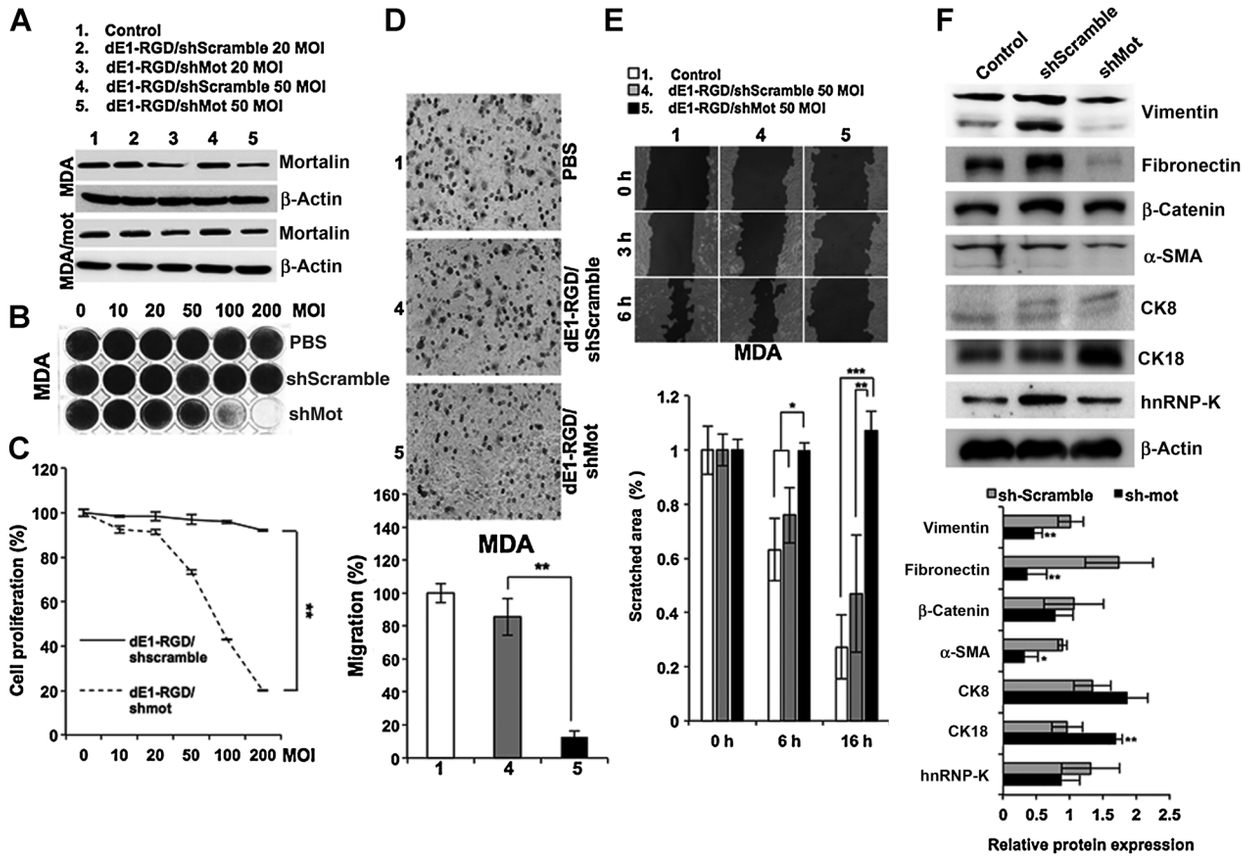


**Figure 6.**
Targeting of mortalin by adeno-oncolytic virus caused reversal of EMT signaling. A, Western blotting of mortalin in control and mortalin-targeting adeno-oncolytic virus at sublethal doses is shown. Cell viability as examined by staining with crystal violet (B); MTT assay (C) showed that the doses 20–50 MOI were sublethal. Cell invasion (D) and migration (E) assays showing decreased migration capacity in mortalin-compromised cells. F, Western blot analysis showing reduction in mesenchymal cell markers and increase in epithelial cell markers in mortalin-compromised cells. Quantitation from three experiments is shown at bottom in panels D–F. Data are presented as mean ± SE ($n = 3$). *, $P < 0.05$; **, $P < 0.01$; ***, $P < 0.001$ compared with untreated or shScramble-treated cells.

examination of cells showed increase in microfilaments (Supplementary Fig. S3). To further validate the contribution of mortalin in cell migration, we generated mortalin-overexpressing human normal fibroblasts (TIG-3). As shown in Supplementary Fig. S4, the latter showed faster migration than the control cells endorsing that the upregulation of mortalin causes an increase in the migration capacity of cells.

### Overexpression of mortalin induces endothelial-to-mesenchymal transition

To unravel the mechanism of role of mortalin in increased migration and invasion of cells, we subjected control and mortalin-overexpressing derivative to cDNA, miRNA, and metastasis-antibody arrays. As shown in Fig. 4A and Supplementary Table S1, cDNA array showed upregulation of focal adhesion, JAK-STAT, and basal cell carcinoma signaling. miRNA array also showed that PI3K–Akt, focal adhesion, cytoskeleton, and TGFβ signaling were affected, at large, in mortalin-overexpressing cells (Fig. 4B). In agreement with these data, mortalin-overexpressing MDA cells showed increase in several key regulators of metastasis and EMT signaling (Fig. 4C, a). Furthermore, conditional medium of mortalin-overexpressing cells showed increased level of expression of metastasis and EMT markers (Fig. 4C, b).

We next validated these findings by gene and protein specific analyses using specific primers and antibodies, respectively. As shown in Fig. 5A and B, Western blotting and immunostaining revealed increase in mesenchymal cell markers including vimentin, fibronectin, β-catenin, hnRNP-K, α-SMA, and CK14. Of note, the epithelial marker proteins, E-cadherin, CK18, and CK8 showed sharp decrease (Fig. 5A and B). In line with the antibody array data, mortalin-overexpressing derivatives showed increase in MMP-2 protein as well as mRNA (Fig. 5C and D). Similar results were obtained for MMP-3 and MMP-9 in mortalin-overexpressing MDA as well as MCF-7 derivatives as compared with their parent control cells (Fig. 5D and Supplementary Fig. S5). We next performed qPCR for the expression of several key genes involved in cell migration, EMT, and metastasis signaling, and found that these genes (MMP-3, MMP-9, hnRNP-K, VEGF, vimentin, Wnt3a, and β-catenin) were upregulated in mortalin-overexpressing derivatives (Fig. 5E). Of note, epithelial cell markers (E-cadherin, CK8) and tumor suppressor TGFβ were decreased in these cells as compared with the control (Fig. 5E). These data supported the role of mortalin in EMT signaling.

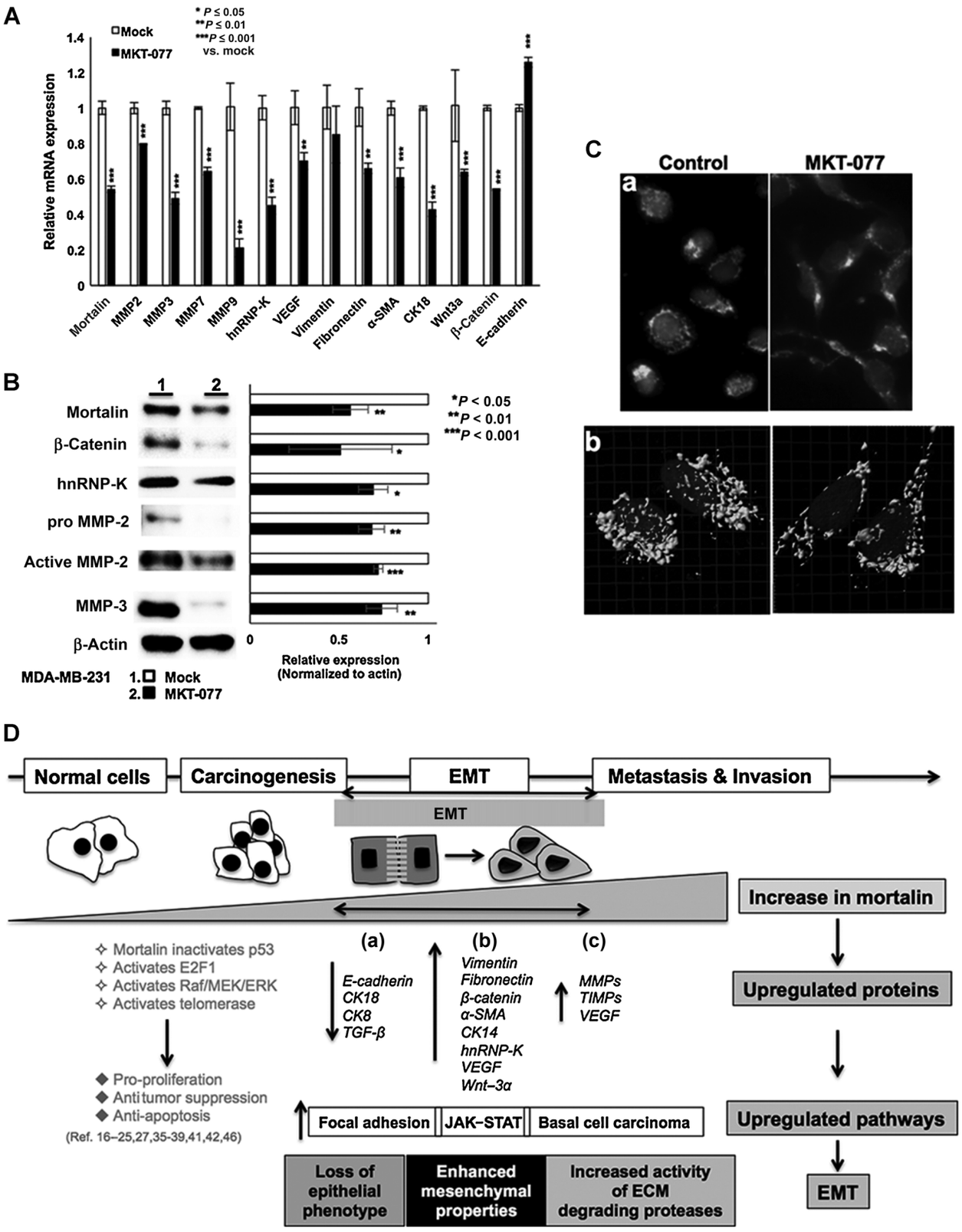

**Mortalin targeting by shRNA-expressing adenovirus leads to reduction in migration and invasion of MDA cells**

To examine whether overexpression was essential for migration or invasion characteristics of cancer cells, we treated the MDA cells and their mortalin-overexpressing derivatives with mortalin-targeting shRNA-expressing adenovirus. The target sequence that has earlier been defined as the most effective one was used for this study (25). Cells were transduced with subtoxic doses (20–50 MOI) of virus. As shown in Fig. 6A–E, we found that at the low subtoxic doses, mortalin-shRNA expressing adenovirus caused significant reduction in cell migration as examined by chemotaxis as well as wound scratch assays (Fig. 6D and E). Of note, although mortalin targeting caused significant reduction in vimentin, fibronectin, and hnRNP-K, CK18 expression increased, suggesting the reversion of EMT in mortalin-compromised cells (Fig. 6F).

**Mortalin targeting by MKT-077 reversed the EMT**

We next used MKT-077 (a mitochondrion-seeking delocalized cationic dye that causes selective death of cancer cells) that was shown to be a chemical inhibitor of mortalin at subtoxic doses (35, 36). It was shown that fairly low drug doses of MKT-077 were sufficient to induce senescence in tumor cells (36). As shown in Fig. 7A and B, MKT-077–treated cells showed significant reduction in proteins crucial for cell migration and EMT. Expression analysis of several genes by qPCR revealed downregulation of MMPs, hnRNP-K, VEGF, vimentin, fibronectin, VEGF, α-SMA, β-catenin, CK18, and Wnt-3α in MKT-077–treated cells; major epithelial cell markers, E-cadherin showed increase. The changes in transcript level were also translated to the protein level (Fig. 7B). In view of our recent findings that the nuclear mortalin leads to aggressive malignant phenotype of cancer cells (23), we examined it in control and MKT-077–treated cells. As shown in Fig. 7C, we found that the latter possessed reduced levels of nuclear mortalin accounting for downregulation of its downstream signaling responsible for malignant transformation of cancer cells.

## Discussion

Metastasis is the major cause of mortality in all the cancer patients. Although primary breast cancer is often treated with surgery and radiation, it is the later stage when cells escape treatment due to chemoresistance and metastasis to the brain, bones, liver, and lungs. Mortalin was shown to activate telomerase, hnRNP-K, E2F1A, and PI3K/AKT proteins (23, 37, 38). In agreement with these known functions of mortalin, it has been detected as an upregulated protein in a variety of human tumors. Cancer genome databases revealed that the renal cell carcinomas (RCC) that accounts for 90% to 95% of malignant neoplasms and 2% to 3% of all malignant diseases in adults most frequently possess amplification of mortalin locus and show high degree of resistance to radiation and chemotherapy. Association of upregulation of mortalin with cancer malignancy and metastasis was also supported by other tumor types as shown in Fig. 2 and Supplementary Fig. S1 and some earlier reports (16, 19, 28, 29). We examined the TCGA database (kidney renal clear cell carcinoma datasets that showed highest frequency of mortalin amplification) for mutual cooccurrence and exclusiveness of mortalin with other proteins. Interestingly, we found tight association of mortalin with FGF1 amplification (Supplementary Fig. S6A and S6B). FGF1 is an established key regulator of cell migration and EMT (39, 40). Mortalin has been reported to interact with FGF1 and to aid in its intracellular trafficking (41, 42), suggesting that this interaction is clinically relevant for carcinogenesis. On the other hand, we found that mortalin amplification and p53 mutations were mutually exclusive (Supplementary Fig. S6B). In contrast to their approximately 70% to 94% occurrence in high-grade epithelial cancers, mortalin-enriched tumor datasets showed extremely low (2%) occurrence of p53 mutation. This was consistent with the earlier established role of mortalin in inactivation of p53 protein and endorsed its clinical relevance. Targeting of mortalin caused growth arrest or apoptosis of cancer cells by activation of p53 signaling (17, 18, 22, 25). However, its relationship with EMT has not been elucidated.

In this study, cDNA and miRNA array analyses in control and mortalin-overexpressing breast epithelial cells revealed upregulation of PI3K–Akt and focal adhesion signaling in the overexpressing derivatives (Fig. 4). PI3K–Akt signaling has been reported to regulate EMT through the transcription factor snail, a critical EMT mediator (43, 44). The proinvasive and prometastasis effects of sorafenib (antiangiogenic agent that inhibits tumor growth but promotes tumor invasion and metastasis in HCC) were assigned to activate PI3K/Akt/snail pathway (45). Overexpression of miR-19a was also shown to activate PI3K/AKT signaling, and induced EMT in gastric cancers (43). Overexpression of mortalin was earlier shown to inactivate p53, activate telomerase, and anti-apoptotic signaling through Raf/MEK/ERK pathway and inhibition of conformational change of Bax (17, 18, 38), and to mediate erythropoietin-induced growth of erythroid progenitor cells (Fig. 7D; ref. 46). It was identified as one of the ten signaling partners of Akt (a serine/threonine kinase) by mass spectrometry analysis (47). Gene-specific analyses indeed revealed activation of EMT in mortalin-overexpressing derivatives (Fig. 7D). These cells showed upregulation of vimentin, fibronectin, α-SMA, CK14, VEGF, Wnt-3α, and hnRNP-K (Fig. 7D). Furthermore, key regulators of metastasis, MMPs, and VEGF showed upregulation at protein as well as transcript levels (Fig. 7D). We found that the mortalin-overexpressing cells possess decreased level of expression of TGFβ tumor suppressor (Fig. 5), a factor that controls cell proliferation, differentiation, and transformation (48). Taken together, in addition to the already accepted role of mortalin in activation of pro-proliferation and antiapoptotic signaling during carcinogenesis, we, in this study, found that it plays a key role in

**Figure 7.**

Targeting mortalin by MKT-077 caused reversal of EMT signaling. A, expression analysis of the indicated genes by qRT-PCR in control and MKT-077–treated cells. B, the level of indicated proteins in control and MKT-077–treated cells as examined by Western blotting. C, immunostaining for mortalin in control and MKT-077–treated cells showing reduction in nuclear mortalin in the latter. Wide-field low magnification (a) and small field high-resolution cross-section (b) images are shown. Nucleus was stained with Hoechst and made transparent by graphic workstation and analyzed with the "Imaris" software (Bitplane). Data are presented as mean ± SE ($n = 3$). *, $P < 0.05$; **, $P < 0.01$; ***, $P < 0.001$ compared with mock. D, schematic diagram showing the role of mortalin in carcinogenesis, EMT, metastasis, and invasion. Increase in mortalin expression in cancer cells caused upregulation of several proteins involved in EMT; whereas, proteins involved in epithelial cell characteristics (a) decreased, the proteins involved in mesenchymal, migration, and invasion characteristics (b and c) showed increase.

EMT by activation of several proteins and pathways (Fig. 7D). The data were validated by mortalin-knockdown using (i) mortalin-specific oncolytic adenovirus and (ii) anti-mortalin small-molecule MKT-077 that resulted in downregulation of several key regulators of EMT both at protein as well as transcript levels (Supplementary Table S1). Of note, E-cadherin, an established marker of epithelial cells, decreased in mortalin-overexpressing cells and increased in MKT-077–treated cells. These data suggested that mortalin works upstream of these factors in regulation of EMT and cancer cells metastasis. Furthermore, only 2- to 3-fold increase in mortalin expression caused increase in migration capacity and activated EMT signaling in a variety of cancer cell lines, such as breast carcinomas (MDA and MCF7), osteosarcoma (U2OS), and melanoma (G361), suggesting that it is a strong regulator and independent of cancer cell types (Supplementary Fig. S4 and S5). We have recently demonstrated that mortalin resides in the nucleus of cancer cells wherein it activates telomerase and hnRNP-K (23), both are related to cancer progression and malignant properties (23, 49, 50). Of note, MKT-077–treated MDA cells showed decrease in nuclear mortalin that may account for downregulation of several proteins involved in EMT (Fig. 7C and D). Together with the results of HCC study (29), the value of mortalin targeting for therapeutic success of aggressive and metastatic cancers is endorsed. Findings suggest that the aberrant enrichment of a stress chaperone protein in multiple tumor types elicits an EMT-like phenotype and promotes the invasiveness of cancer cells, warranting further investigation as a potentially broad-acting therapeutic target.

## Disclosure of Potential Conflicts of Interest

No potential conflicts of interest were disclosed

## Authors' Contributions

**Conception and design:** S.C. Kaul, J.-S. Lee, C.-O. Yun, R. Wadhwa
**Development of methodology:** Y. Na, J.-S. Lee, R. Wadhwa
**Acquisition of data (provided animals, acquired and managed patients, provided facilities, etc.):** Y. Na, J. Ryu, Z. Kaul, R.S. Kalra, L. Li, C.-O. Yun
**Analysis and interpretation of data (e.g., statistical analysis, biostatistics, computational analysis):** Y. Na, S.C. Kaul, J. Ryu, H.M. Ahn, R.S. Kalra, L. Li, N. Widodo, C.-O. Yun, R. Wadhwa
**Writing, review, and/or revision of the manuscript:** S.C. Kaul, R. Wadhwa
**Administrative, technical, or material support (i.e., reporting or organizing data, constructing databases):** S.C. Kaul, R. Wadhwa
**Study supervision:** S.C. Kaul, R. Wadhwa

## Acknowledgments

The authors thank Anupama Chaudhary and Seong Kyung Lee for technical assistance.

## Grant Support

This work was supported by grants from the National Institute of Advanced Industrial Science & Technology (AIST)-DAILAB Special Fund (S.C. Kaul and R. Wadhwa) and National Research Foundation of Korea (2010-0029220, 2013K1A1A2A02050188, and 2013M3A9D3045879 to C.-O. Yun).

The costs of publication of this article were defrayed in part by the payment of page charges. This article must therefore be hereby marked *advertisement* in accordance with 18 U.S.C. Section 1734 solely to indicate this fact.

Received October 6, 2015; revised January 8, 2016; accepted January 20, 2016; published OnlineFirst March 9, 2016.

## References

1. Cano A, Perez-Moreno MA, Rodrigo I, Locascio A, Blanco MJ, del Barrio MG, et al. The transcription factor snail controls epithelial-mesenchymal transitions by repressing E-cadherin expression. Nat Cell Biol 2000;2:76–83.
2. Wang Y, Shi J, Chai K, Ying X, Zhou BP. The role of snail in EMT and tumorigenesis. Curr Cancer Drug Targets 2013;13:963–72.
3. Mallini P, Lennard T, Kirby J, Meeson A. Epithelial-to-mesenchymal transition: what is the impact on breast cancer stem cells and drug resistance. Cancer Treat Rev 2014;40:341–8.
4. Yi BR, Kim TH, Kim YS, Choi KC. Alteration of epithelial-mesenchymal transition markers in human normal ovaries and neoplastic ovarian cancers. Int J Oncol 2015;46:272–80.
5. Mironchik Y, Winnard PTJr, Vesuna F, Kato Y, Wildes F, Pathak AP, et al. Twist overexpression induces *in vivo* angiogenesis and correlates with chromosomal instability in breast cancer. Cancer Res 2005;65:10801–9.
6. Tania M, Khan MA, Fu J. Epithelial to mesenchymal transition inducing transcription factors and metastatic cancer. Tumour Biol 2014;35:7335–42.
7. Su J, Yin X, Zhou X, Wei W, Wang Z. The functions of F-box proteins in regulating the epithelial to mesenchymal transition. Curr Pharm Des 2015;21:1311–7.
8. Micalizzi DS, Farabaugh SM, Ford HL. Epithelial-mesenchymal transition in cancer: parallels between normal development and tumor progression. J Mammary Gland Biol Neoplasia 2010;15:117–34.
9. Xiong X, Wang Y, Liu C, Lu Q, Liu T, Chen G, et al. Heat shock protein 90beta stabilizes focal adhesion kinase and enhances cell migration and invasion in breast cancer cells. Exp Cell Res 2014;326:78–89
10. Bokhari AA, Syed V. Inhibition of transforming growth factor-beta (TGF-beta) signaling by Scutellaria baicalensis and Fritillaria cirrhosa extracts in endometrial cancer. J Cell Biochem 2015;116:1797–805.
11. Zarzynska JM. Two FACes of TGF-beta1 in breast cancer. Mediators Inflamm 2014;2014:141747.
12. Chang CJ, Chao CH, Xia W, Yang JY, Xiong Y, Li CW, et al. p53 regulates epithelial-mesenchymal transition and stem cell properties through modulating miRNAs. Nat Cell Biol 2011;13:317–23.
13. Hiscox S, Morgan L, Barrow D, Dutkowskil C, Wakeling A, Nicholson RI, et al. Tamoxifen resistance in breast cancer cells is accompanied by an enhanced motile and invasive phenotype: inhibition by gefitinib ('Iressa', ZD1839). Clin Exp Metastasis 2004;21:201–12.
14. Krasnapolski MA, Todaro LB, de Kier Joffe EB. Is the epithelial-to-mesenchymal transition clinically relevant for the cancer patient? Current Pharm Biotechnol 2011;12:1891–9.
15. Zhang P, Liu H, Xia F, Zhang QW, Zhang YY, Zhao Q, et al. Epithelial-mesenchymal transition is necessary for acquired resistance to cisplatin and increases the metastatic potential of nasopharyngeal carcinoma cells. Int J Mol Med 2014;33:151–9.
16. Wadhwa R, Takano S, Kaur K, Deocaris CC, Pereira-Smith OM, Reddel RR, et al. Upregulation of mortalin/mthsp70/Grp75 contributes to human carcinogenesis. Int J Cancer 2006;118:2973–80.
17. Lu WJ, Lee NP, Kaul SC, Lan F, Poon RT, Wadhwa R, et al. Mortalin-p53 interaction in cancer cells is stress dependent and constitutes a selective target for cancer therapy. Cell Death Differ 2011;18:1046–56.
18. Lu WJ, Lee NP, Kaul SC, Lan F, Poon RT, Wadhwa R, et al. Induction of mutant p53-dependent apoptosis in human hepatocellular carcinoma by targeting stress protein mortalin. Int J Cancer 2011;129:1806–14.
19. Ando K, Oki E, Zhao Y, Ikawa-Yoshida A, Kitao H, Saeki H, et al. Mortalin is a prognostic factor of gastric cancer with normal p53 function. Gastric Cancer 2014;17:255–62.
20. Wadhwa R, Takano S, Robert M, Yoshida A, Nomura H, Reddel RR, et al. Inactivation of tumor suppressor p53 by mot-2, a hsp70 family member. J Biol Chem 1998;273:29586–91.
21. Ma Z, Izumi H, Kanai M, Kabuyama Y, Ahn NG, Fukasawa K. Mortalin controls centrosome duplication via modulating centrosomal localization of p53. Oncogene 2006;25:5377–90.
22. Kaul SC, Aida S, Yaguchi T, Kaur K, Taira K, Wadhwa R, et al. .Activation of wild type p53 function by its mortalin-binding cytoplasmically localizing carboxy-terminus peptides. J Biol Chem 2005;280:39373–9.
23. Ryu J, Kaul Z, Yoon AR, Liu Y, Yaguchi T, Na Y, et al. Identification and functional characterization of nuclear mortalin in human carcinogenesis. J Biol Chem 2014;289:24832–44.

24. Wadhwa R, Ando H, Kawasaki H, Taira K, Kaul SC. Targeting mortalin using conventional and RNA-helicase-coupled hammerhead ribozymes. EMBO Rep 2003;4:595–601.
25. Yoo JY, Ryu J, Gao R, Yaguchi T, Kaul SC, Wadhwa R, et al. Tumor suppression by apoptotic and anti-angiogenic effects of mortalin-targeting adeno-oncolytic virus. J Gene Med 2010;12:586–95.
26. Benbrook DM, Nammalwar B, Long A, Matsumoto H, Singh A, Bunce RA, et al. SHetA2 interference with mortalin binding to p66shc and p53 identified using drug-conjugated magnetic microspheres. Invest New Drugs 2014;32:412–23.
27. Sane S, Abdullah A, Boudreau DA, Autenried RK, Gupta BK, Wang X, et al. Ubiquitin-like (UBX)-domain-containing protein, UBXN2A, promotes cell death by interfering with the p53-Mortalin interactions in colon cancer cells. Cell Death Dis 2014;5:e1118
28. Yi X, Luk JM, Lee NP, Peng J, Leng X, Guan XY, et al. Association of mortalin (HSPA9) with liver cancer metastasis and prediction for early tumor recurrence. Mol Cell Proteomics 2008;7:315–25.
29. Chen J, Liu WB, Jia WD, Xu GL, Ma JL, Huang M, et al. Overexpression of Mortalin in hepatocellular carcinoma and its relationship with angiogenesis and epithelial to mesenchymal transition. Int J Oncol 2014;44:247–55.
30. Yoo JY, Kim JH, Kim J, Huang JH, Zhang SN, Kang YA, et al. Short hairpin RNA-expressing oncolytic adenovirus-mediated inhibition of IL-8: effects on antiangiogenesis and tumor growth inhibition. Gene Ther 2008;15: 635–51.
31. Vlachos IS, Kostoulas N, Vergoulis T, Georgakilas G, Reczko M, Maragkakis M, et al. DIANA miRPath v.2.0: investigating the combinatorial effect of microRNAs in pathways. Nucleic Acids Res 2012;40:W498–504.
32. Chang JT, Nevins JR. GATHER: a systems approach to interpreting genomic signatures. Bioinformatics 2006;22:2926–33
33. Draghici S, Khatri P, Tarca AL, Amin K, Done A, Voichita C, et al. A systems biology approach for pathway level analysis. Genome Res 2007;17:1537–45.
34. Kanehisa M, Goto S. KEGG: kyoto encyclopedia of genes and genomes. Nucleic Acids Res 2000;28:27–30.
35. Wadhwa R, Sugihara T, Yoshida A, Nomura H, Reddel RR, Simpson R, et al. Selective toxicity of MKT-077 to cancer cells is mediated by its binding to the hsp70 family protein mot-2 and reactivation of p53 function. Cancer Res 2000;60:6818–21.
36. Deocaris CC, Widodo N, Shrestha BG, Kaur K, Ohtaka M, Yamasaki K, et al. Mortalin sensitizes human cancer cells to MKT-077-induced senescence. Cancer Lett 2007;252:259–69.
37. Wadhwa R, Ryu J, Ahn HM, Saxena N, Chaudhary A, Yun CO, et al. Functional significance of point mutations in stress chaperone mortalin and their relevance to Parkinson disease. J Biol Chem 2015;290:8447–56.
38. Yang L, Guo W, Zhang Q, Li H, Liu X, Yang Y, Zuo J, et al. Crosstalk between Raf/MEK/ERK and PI3K/AKT in suppression of Bax conformational change by Grp75 under glucose deprivation conditions. J Mol Biol 2011;414:654–66.
39. Smith G, Ng MTH, Shepherd L, Herrington CS, Gourley C, Ferguson MJ, et al. Individuality in FGF1 expression significantly influences platinum resistance and progression-free survival in ovarian cancer. Br J Cancer 2012;107:1327–36.
40. Shi H, Fu C, Wang W, Li Y, Du S, Cao R, et al. The FGF-1-specific single-chain antibody scFv1C9 effectively inhibits breast cancer tumour growth and metastasis. J Cell Mol Med 2014;18:2061–70.
41. Mizukoshi E, Suzuki M, Loupatov A, Uruno T, Hayashi H, Misono T, et al. Fibroblast growth factor-1 interacts with the glucose-regulated protein GRP75/mortalin. Biochem J 1999;343:461–6.
42. Mizukoshi E, Suzuki M, Misono T, Loupatov A, Munekata E, Kaul SC, et al. Cell-cycle dependent tyrosine phosphorylation on mortalin regulates its interaction with fibroblast growth factor-1. Biochem Biophys Res Commun 2001;280:1203–9.
43. Lu W, Xu Z, Zhang M, Zuo Y. MiR-19a promotes epithelial-mesenchymal transition through PI3K/AKT pathway in gastric cancer. Int J Clin Exp Pathol 2014;7:7286–96.
44. Wang Y, Shi J, Chai K, Ying X, Zhou BP. The role of snail in EMT and tumorigenesis. Curr Cancer Drug Targets 2013;13:963–72.
45. Wang H, Xu L, Zhu X, Wang P, Chi H, Meng Z, et al. . Activation of phosphatidylinositol 3-kinase/Akt signaling mediates sorafenib-induced invasion and metastasis in hepatocellular carcinoma. Oncol Rep 2014;32: 1465–72.
46. Ohtsuka R, Abe Y, Fujii T, Yamamoto M, Nishimura J, Takayanagi R, et al. Mortalin is a novel mediator of erythropoietin signaling. Eur J Haematol 2007;79:114–25.
47. Vandermoere F, El Yazidi-Belkoura I, Demont Y, Slomianny C, Antol J, Lemoine J, et al. Proteomics exploration reveals that actin is a signaling target of the kinase Akt. Mol Cell Proteomics 2007;6:114–24.
48. Moustakas A, Heldin P. TGFbeta and matrix-regulated epithelial to mesenchymal transition. Biochim Biophys Acta 2014;1840:2621–34.
49. Makki J, Myint O, Wynn AA, Samsudin AT, John DV. Expression distribution of cancer stem cells, epithelial to mesenchymal transition, and telomerase activity in breastcancer and their association with clinicopathologic characteristics. Clin Med Insights Pathol 2015;8: 1–16.
50. Gao R, Yu Y, Inoue A, Widodo N, Kaul SC, Wadhwa R. Heterogeneous nuclear ribonucleoprotein K (hnRNP-K) promotes tumor metastasis by induction of genes involved in extracellular matrix, cell movement, and angiogenesis. J Biol Chem 2013;288:15046–56.